Two-parameter FCG driving force: successive blocking of the monotonic and cyclic plastic zones at microstructural barriers

C. Vallellano
Department of Mechanical and Material Engineering,University of Sevilla, Sevilla (Spain)
carpofor@us.es

A. Navarro
Department of Mechanical and Material Engineering,University of Sevilla, Sevilla (Spain)
navarro@us.es

J. Dominguez
Department of Mechanical and Material Engineering,University of Sevilla, Sevilla (Spain)
jaime@us.es

ABSTRACT. A micromechanical description of small fatigue crack growth based on the successive blocking of the monotonic plastic zone (MPZ) and cyclic plastic zone (CPZ) of a crack at microstructural barriers such as grain boundaries and phase limits is presented. The model allows two different fatigue crack growth thresholds to be established, one of which, the *maximum-controlled fatigue threshold*, is dependent on the capability of MPZ to overcome successive material barriers and the other, the *range-controlled fatigue threshold*, is associated with the capability of CPZ to overcome such barriers as well. The implications of this micromechanical model and its applicability depending on the loading conditions are discussed, linking and supporting in a natural manner with use of two-parameter crack driving force ($\Delta K - K_{\max}$) to characterize the fatigue crack growth in the long crack regime.

KEYWORDS. Small cracks; Two-parameters; Fatigue crack growth; Fatigue thresholds

INTRODUCTION

There is nowadays a growing trend to describe fatigue crack driving force by means of models based on two independent parameters, one related to the applied load range (*e.g.* $\Delta\sigma$, ΔK) and the other associated to the maximum load level (*e.g.* $\sigma_{\max}$, $K_{\max}$). These models seem to rely on the fatigue crack growth description proposed by Vasudevan and co-workers [1-3], which propose two independent stress intensity factors threshold ΔK_{th}^{*} and $K_{\max,th}^{*}$ for the long crack regime. Such two-parameter models seem to be very promising. However, most of reported approaches are purely phenomenological and are focused on long cracks. Some of them propose a crack driving force depending on additive functions of $K_{\max}$ and ΔK [4], but most of them assume a multiplicative relationship ($da/dN \sim \Delta K^{m} \cdot K_{\max}^{n}$) [5-10]. Recently, Shyam et al. [11] have developed a phenomenological small crack growth model based on the separate contributions of cyclic and monotonic plasticity to the crack propagation process. The crack growth rate is assumed to be

linearly related to the product of the monotonic and cyclic crack-tip opening displacements, ϕ_{max} and $\Delta\phi$ respectively, that is, $da/dN \sim \Delta\phi \cdot \phi_{max}$.

In a recent publication, the authors have presented a micromechanical description of small fatigue crack growth based on the successive blocking of the monotonic plastic zone (MPZ) and cyclic plastic zone (CPZ) of a crack at microstructural barriers such as grain boundaries and phase limits [12]. The mathematical formulation of the present model is based on the fatigue crack growth description by Navarro and de los Rios [13-15]. The model allows two different fatigue crack growth thresholds to be established, one of which, the *maximum-controlled fatigue threshold*, is dependent on the capability of MPZ to overcome successive material barriers and the other, the *range-controlled fatigue threshold*, is associated with the capability of CPZ to overcome such barriers as well. The present paper discusses the implications of this micromechanical model and its applicability depending on the loading conditions, linking in a natural manner with recent advances in fatigue mechanics relying on the use of two-parameter crack driving force ($\Delta K - K_{max}$) in the long cracks regime.

CONCEPTUAL MODEL

The crack propagation description relies on the assumption that, at the microscopic level, fatigue cracks interact continuously with the microstructure of the material, and this interaction consist mainly in successive and continuous blocks of its plastics zones at the microstructural barriers. Two pioneering works exploiting this idea were put forward by Takana and coworkers [16,17] and Navarro and de los Rios [13-15]. Briefly, and among other differences, the former employs the interaction of the CPZ to characterize the growth of small fatigue cracks, whereas the latter makes use of the interaction of the MPZ to describe the fatigue crack propagation process.

The original NR model assumes the MPZ of the crack to advance by blocking at the successive microstructural barriers in the material. Thus, a crack will only propagate beyond a barrier if it can trigger plastic slip in a neighbouring grain; otherwise, the crack will not be able to overcome the barrier and it will arrest at it. The nucleation process of plastic slip has to be repeated afresh in each grain. In these situations, it makes sense to assume that dislocations are constrained (e.g. by stacking fault energy) to remain on their original planes and pile up against grain boundaries, giving rise to rectilinear slip bands extending through the successive grains.

The present model extends the original fatigue crack growth description given by Navarro and de los Rios by introducing the additional assumption that the CPZ can also be blocked by the microstructural barriers. Admittedly, at this stage, the experimental support of this assumption is not an easy task. However, we believe it is worth while exploring its consequences. Thus, the capability of both MPZ and CPZ to overcome, or not, the successive barriers determines the capability of the crack to propagate up to fatigue failure, or to get arrested at a certain microstructural barrier, becoming a non-propagating crack. This point of view allows one to establish two independent threshold conditions for fatigue crack growth. It can be readily inferred that the former threshold condition should be controlled by the maximum applied load, and the latter one should be managed by the applied load range, or a certain effective load range.

Following the ideas above and to summarize, the proposed model is developed in accordance with the following working hypothesis:

1. Microstructural features in the material such as grain boundaries, phase limits or inclusions act as barriers against plastic slip and hinder expansion of both the monotonic plastic zone (MPZ) and cyclic plastic zone (CPZ) in front of the crack.
2. The expansion of the MPZ beyond a given barrier depends on its capability to produce plastic slip beyond the barrier, which in turn depends on the maximum applied load (*e.g.* σ_{max}, K_{max}).
3. The CPZ always expands within MPZ, and its size depends on the applied load range (*e.g.* $\Delta\sigma$, ΔK, $\Delta\phi$, etc.). Microstructural barriers within MPZ, previously overcome by MPZ, act as barriers for CPZ as well. The ability of CPZ to overcome such barriers depends on the applied load range (*e.g.* $\Delta\sigma$, ΔK, $\Delta\phi$, etc.).
4. No fatigue crack can propagate in the absence of a CPZ in its front. This seems a natural assumption since it is inside the CPZ where cyclic damage is more intense due to the effect of the irreversibility of the dislocation motion and the accumulation and/or the annihilation of dislocations during the cyclic loading.
5. As a consequence, the crack growth rate, da/dN, should be a function of the range of the applied loads or their associated variables (*e.g.* $\Delta\sigma$, ΔK, $\Delta\phi$, etc.). Since the crack tip opening displacement range is a variable more sensitive to microstructure when the crack is small, it is assumed in this work that da/dN is a function of $\Delta\phi$.

MATHEMATICAL FORMULATION

By using distributed dislocation techniques a crack, its plastic zones and the barrier zone can be modeled [15,18]. Edge dislocations, occurring in the crack plane and with Burgers vectors in the pane too (see Fig. 1), allow opening mode II to be simulated, while dislocations with Burgers vectors normal to the crack plane allow opening mode I to be modelled. Mode III can be modelled by using screw dislocations.

Fig. 1 represents a crack of length $2a$ growing through a given number of grains in a polycrystal subjected to the maximum stress of the cycle, and its MPZ blocked at a certain barrier i. For simplicity, the grain size will be assumed to be constant and equal to D; also, we shall assume the grain boundaries to be the sole microstructural barriers opposing crack growth. The index of the barrier i is an odd integer number ($i = 1,3,5,...$), so that $iD/2$ gives the theoretical position of each successive barrier (see Fig. 1 for nomenclature). In general, the crack is under a stress σ_1^i opposing opening of its sides. This stress is usually assumed to be negligible. The monotonic plastic zone (MPZ), which runs from the crack tip to the barrier at which it is blocked, is sustaining a stress σ_2^i opposing plastic slip in front of the crack. This stress, also referred to in the literature as "friction stress", represents the local yield strength of the plastic zone, *i.e.* the local resistance to motion of dislocations in plastic zone. Initially, when the MPZ is embedded in the first grain, σ_2^1 is similar to the yield stress for a monocrystal. This yield stress will increase as the MPZ incorporates an increasing number of randomly oriented grains. Thus, when such a number is large enough, the average mechanical properties of MPZ are similar to those of a polycrystal [19], *i. e.* $\sigma_2^\infty \approx \sigma_Y$, where σ_Y represents the macroscopic yield strength of the polycrystalline material. The evolution of the local yield strength of the plastic zone has been analyzed in detail by Chan and Lankford [20]. For instance, a ratio of σ_Y / σ_2^1 around 4 is suggested for a 7075 Aluminum Alloy. Fig. 2 shows the progression of σ_2^i as a function of the plastic zone length proposed by Chan and Lankford and a more gradual approach used by the current author for an aluminum alloy [12].

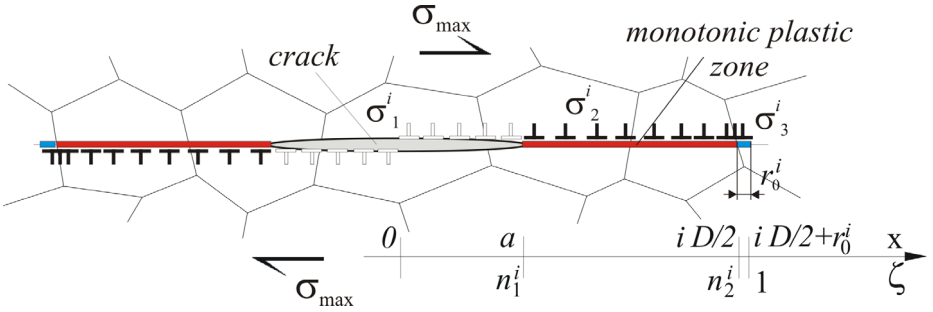

Figure 1: Schematic representation of the crack, MPZ and barrier zone at the maximum stress of the cycle (mode II).

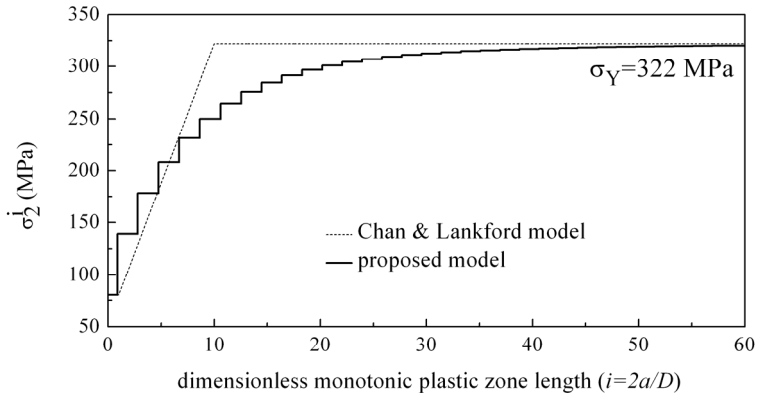

Figure 2: Evolution of stress local yield stress σ_2^i versus the MPZ size.

Finally, the barrier is assumed to be a small additional zone of length r_0^i ($r_0^i \ll D$) representing the typical size of the interface between neighbouring grains or the phases, or the width of distance to dislocations sources. This zone is assumed to be under a stress σ_3^i representing the pressure exerted by dislocations in MPZ on the microstructural barrier. The solution of this distribution of dislocations, sometimes referred to as a *bounded solution*, is very well known in the literature, (see [15,18] for details). Under the assumptions $\sigma_1^i \approx 0$ and $n_2^i \approx 1$, the force balance in each dislocation will be reached when the so-called *existence condition* is fulfilled

$$\frac{\pi}{2}\sigma_{\max} - \sigma_2^i \cos^{-1} n_1^i = \sigma_3^i \cos^{-1} n_2^i \tag{1}$$

where $n_1^i \approx a/iD/2$ represents the ratio of the crack length versus the MPZ size. Note that Eq. (1) allows the calculation of σ_3^i as a function of the stress σ_2^i, the crack length, barrier width r_0^i and applied stress. This will be used later to formulate the threshold conditions. Finally, the crack tip opening displacement at the peak of the cycle (*i.e.* at $\sigma_{\max}$) can be approximated assuming $r_0^i \to 0$ as (see [13-15]).

$$\phi_{\max}^i = \frac{8}{\pi^2 E'}\frac{K_{\max}^2}{\sigma_{\max}}\left\{\left(\frac{\sigma_2^i}{\sigma_{\max}}\right)\ln\left(\frac{1}{n_1^i}\right) + \frac{\pi}{2}\frac{\sqrt{1-(n_1^i)^2}}{n_1^i}\left[1 - \frac{2}{\pi}\left(\frac{\sigma_2^i}{\sigma_{\max}}\right)\cos^{-1} n_1^i\right]\right\} \tag{2}$$

where $K_{\max} = \sigma_{\max}\sqrt{\pi a}$; and $E' = E/(1-\nu^2)$ in plane strain and $E' = E$ in plane stress.
As soon as unloading begins, the cyclic plastic zone (CPZ) is formed at the crack tip within the monotonic plastic zone (MPZ), that expands in proportion to the load range ($\Delta\sigma$). The CPZ encompasses two kinds of dislocations. On the one hand, those dislocations originally in MPZ whose motion can be reversed due to decreased load and can, thus, move back to the crack tip. On the other hand, the new dislocations emanated from the crack tip of opposite sign to the original dislocations. Note that both kinds of dislocations are mathematically equivalent, and they configure a net distribution of dislocations in the CPZ of opposite sign to those dislocations originally created in the MPZ (see Fig. 3). Of course, in a real situation a dislocation annihilation process would have also taken place to configure this final net dislocation distribution. However, this process is not taken into account in the present model.

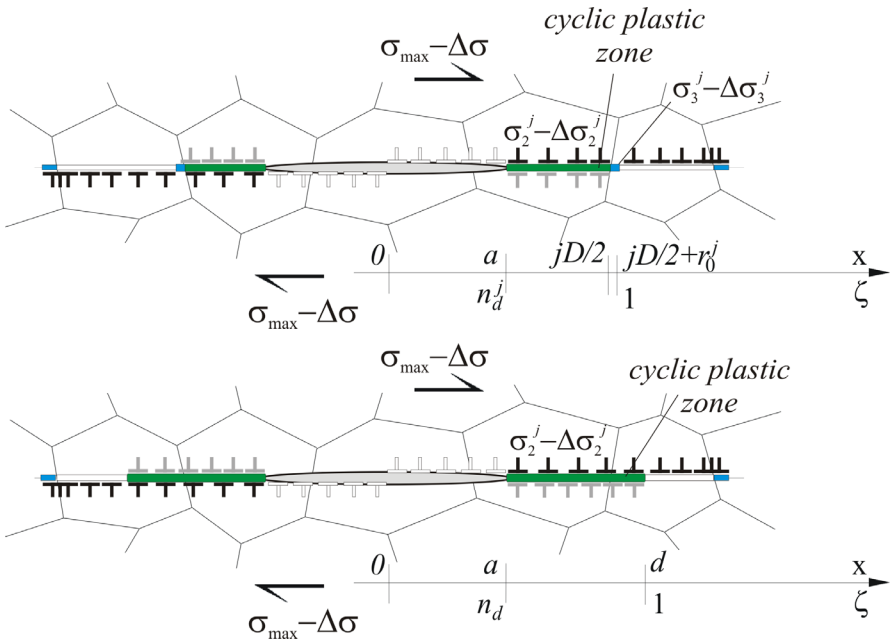

Figure 3: Schematic representation of the crack and CPZ during the unloading process (mode II): CPZ blocked at a microstructural barrier (top) and CPZ in equilibrium within a grain (bottom).

In the unloading process, it is also considered that microstructural barriers block the progress of CPZ. Thus, two situations can be differentiated now: (a) the CPZ blocked at a microstructural barrier within the MPZ (Fig. 3-top), and (b) the CPZ beyond a certain barrier and in equilibrium within a grain before reaching the next barrier. (Fig. 3-bottom). In the first case, the CPZ is blocked by a generic barrier j within the MPZ such that $j \le i$. This situation is similar to that prevailing at the maximum load. The equilibrium of dislocations will therefore fulfilled by replacing σ by $\Delta\sigma$ in Eq. (1), that is,

$$\frac{\pi}{2}\Delta\sigma - \Delta\sigma_2^j \cos^{-1} n_d^j = \Delta\sigma_3^j \cos^{-1} n_2^j \tag{3}$$

where $n_d^j \approx a/jD/2$ represents now the ratio of the crack length versus the CPZ size and $n_2^j \approx 1$. As before, Eq. (3) allows calculation of $\Delta\sigma_3^i$ as a function of the stress $\Delta\sigma_2^i$, the crack length, barrier width r_0^i and the range of the applied stress. The stress $\Delta\sigma_2^j$ is the variation in the local yield stress required to reverse plastic flow for a CPZ just before overcoming a generic barrier j within the MPZ ($j \le i$). Assuming a perfectly plastic material behaviour, the reversal local yield stress $\Delta\sigma_2^j$ can be as twice the monotonic yield stress at the same barrier j, *i.e.* $\Delta\sigma_2^j \approx 2\sigma_2^j$. This yields an evolution of $\Delta\sigma_2^j$ similar to the one given in Fig. 2. Finally, the stress $\Delta\sigma_3^j$ simulates the 'pressure' variation exerted by dislocations in the CPZ on the barrier j.

It can be readily seen that, for the case of a CPZ in equilibrium within a grain (case (b)), the dislocation in CPZ must be balanced with the applied stress when the following *existence condition* is obeyed:

$$\frac{\pi}{2}\Delta\sigma - \Delta\sigma_2^j \cos^{-1} n_d = 0 \quad \rightarrow \quad n_d = \frac{a}{d} = \cos\left(\frac{\pi}{2}\frac{\Delta\sigma}{\Delta\sigma_2^j}\right) \tag{4}$$

where n_d is the dimensionless crack length and d is the current position of the tip of CPZ. The Eq. (4) is used to calculate the value of d as a function of the current crack length, the reversal friction stress $\Delta\sigma_2^i$ and the range of the applied stress. Note that in the previous case, the position of the CPZ was known beforehand, *i.e.* $d = jD/2$.

The expression for the crack tip opening displacement range can be obtained from Eq. (2), simply by replacing maximum values with range values and n_1^i with n_d.

$$\Delta\phi^j = \frac{8}{\pi^2 E'}\frac{\Delta K^2}{\Delta\sigma}\left\{\left(\frac{\Delta\sigma_2^j}{\Delta\sigma}\right)\ln\left(\frac{1}{n_d}\right) + \frac{\pi}{2}\frac{\sqrt{1-(n_d)^2}}{n_d}\left[1 - \frac{2}{\pi}\left(\frac{\Delta\sigma_2^j}{\Delta\sigma}\right)\cos^{-1} n_d\right]\right\} \tag{5}$$

where $n_d = a/d$ is given by Eq. (3) for a CPZ within a grain or $n_d = n_d^j = a/jD/2$ for a CPZ blocked at the j-th microstructural barrier.

Assuming the superposition principle can be applied, the CTOD at the minimum stress of the cycle can be calculated by subtracting the CTOD range from the CTOD at the maximum, $\phi_{\min}^i = \phi_{\max}^i - \Delta\phi^j$.

Threshold Conditions for small cracks

Based on assumptions (*a*) and (*e*) in our working hypotheses, a fatigue crack will arrest when no CPZ exists in front of it. This will occur in two situations: (I) if CPZ fails to overcome some microstructural barrier as it evolves within the MPZ, or (II) if MPZ fails to overcome a given microstructural barrier. In the former case, the CPZ will progress until it blocks at that particular barrier within the MPZ, depleting it form dislocations progressively until the crack propagation capability is annulled as a result. In the latter case, even if CPZ is able to overcome all barriers within MPZ, if the MPZ is blocked at a certain barrier, then the crack will sooner or later reach such a barrier, eliminating its CPZ and stopping. These two situations allow two distinct fatigue growth threshold conditions to be established.

The maximum-controlled fatigue threshold

This threshold refers to a condition of permanent blocking of the MPZ, which would end up with the crack arrest according to the situation (II).

As in earlier models [15], MPZ is assumed to expand stepwise by effect of its being blocked at successive microstructural barriers. The dimensionless critical crack length $n_1^i\big|_C \approx a_C^i / iD/2$ needed to overcome a certain barrier i at a given maximum applied stress $\sigma_{\max}$ is given by [12,15]

$$n_1^i\big|_C = \cos\left(\frac{\pi}{2}\frac{\sigma_{\max}-\sigma_{thi}^*}{\sigma_2^i}\right) \tag{6}$$

where σ_{thi}^* is the maximum threshold stress for a small crack to overcome a generic microstructural barrier i. The Eq. (6) can also be expressed in terms of the maximum SIF as follows:

$$n_1^i\big|_C = \cos\left(\frac{\pi}{2}\frac{\sigma_{\max}}{\sigma_2^i}\left(1-\frac{K_{thi}^*}{K_{\max}}\right)\right) \tag{7}$$

where K_{thi}^* represents the maximum threshold SIF for a small crack blocked at the barrier i ($K_{thi}^* = \sigma_{thi}^*\sqrt{\pi a}$). According to these equations, the crack will only propagate beyond the i-th barrier, if $\sigma_{\max} \geq \sigma_{thi}^*$ or $K_{\max} \geq K_{thi}^*$. In practice, the evolution of σ_{thi}^* or K_{thi}^* with crack length is obtained from the well-known Kitagawa-Takahashi diagram for the material. In the absence of experimental data, semi-empirical expressions can be used, see for instance [21, 22].

As can be inferred either Eq. (6) or Eq. (7), the capability of the MPZ to overcome a microstructural barrier depends exclusively on the maximum applied stress or maximum SIF. Accordingly, this threshold shall be referred as a *maximum-controlled fatigue threshold.*

The range-controlled fatigue threshold

As noted earlier, the CPZ propagates within the MPZ, where grain boundaries act as microstructural barriers opposing its expansion as well. Unlike the previous case, dislocations in CPZ face resistance to motion not only from the material barrier, but also from existing dislocations in MPZ, which may be able to retain them at equilibrium before they reach some microstructural barrier. Thus, it is now assumed that the CPZ is able to expand in a sustained manner *within* a grain: whereas the end of the MPZ will always be blocked at the barrier, that of the CPZ may be located anywhere within the grain. In this case, the size of CPZ is obtained via Eq. (4).

As the crack propagates and CPZ progresses with it, CPZ will successively reach the microstructural barriers in MPZ. The resistance to plastic slip of these barriers will arise mainly from the crystallographic misorientation between neighbouring grains or phases. At this point, it can be hypothesized that the overall resistance of the barrier might be diminished in some way, because the dislocation sources have been already activated during the previous loading process. Once the barrier is overcome, CPZ will suddenly expand until it is retained again, either by dislocations in MPZ or by the next barrier.

Similarly to the previous case, the dimensionless critical crack length $n_d^j\big|_C \approx a_C^j / jD/2$ needed to overcome a generic barrier j at a given rage of applied stress $\Delta\sigma$ is given by [12]

$$n_d^j\big|_C = \cos\left(\frac{\pi}{2}\frac{\Delta\sigma-\Delta\sigma_{thi}^*}{\Delta\sigma_2^j}\right) \tag{8}$$

where $\Delta\sigma_{thj}^*$ is the threshold stress range for a small crack to overcome a generic microstructural barrier j. In terms of the SIF range, Eq. (8) can be rearranged as

$$n_d^j\big|_C = \cos\left(\frac{\pi}{2}\frac{\Delta\sigma}{\Delta\sigma_2^j}\left(1-\frac{\Delta K_{thj}^*}{\Delta K}\right)\right) \tag{9}$$

where ΔK_{thj}^* represents the threshold SIF range for a small crack to overcome a generic barrier j. Again, the evolution of $\Delta\sigma_{thj}^*$ or ΔK_{thj}^* should be estimated experimental or semi-empirically via the Kitagawa-Takahashi diagrams.

Finally, from the stress range point of view, for a crack to propagate beyond a generic barrier i, the crack and its CPZ must be able to overcome every single j barrier ($j \leq i$). This crack growth threshold condition can be expressed as

$\Delta K^*_{thi} \equiv \max_{j \le i} \left\{ \Delta K^*_{thj} \right\}$, where ΔK^*_{thi} represents the threshold SIF range for a small crack to overcome the barrier i. As before, this threshold shall be referred as the *range-controlled fatigue threshold.*

Giving that both the *maximum-controlled fatigue threshold* and the *range-controlled fatigue threshold* are associated to different events, both must be satisfied independently to ensure a small crack grows by fatigue. Thus, a propagation region and an arrest region for small cracks can be defined at every microstructural barrier in a $\Delta K - K_{\max}$ diagram (see Fig. 4(left)). This evolution is quite consistent with the experimental trend observed for long cracks. In fact, Figure 4 (center and right) depicts the experimental results from different authors and different materials showing the existence of two independent SIF thresholds for long cracks, one is related with a maximum SIF value and other related with a range of the SIF. According to Vasudevan *et al.* [1,2] the maximum threshold SIF for long cracks ($K^*_{th\infty}$) causes what they call a 'static damage' in the material, and the threshold SIF range ($\Delta K^*_{th\infty}$) accounts for a 'cyclic damage'.

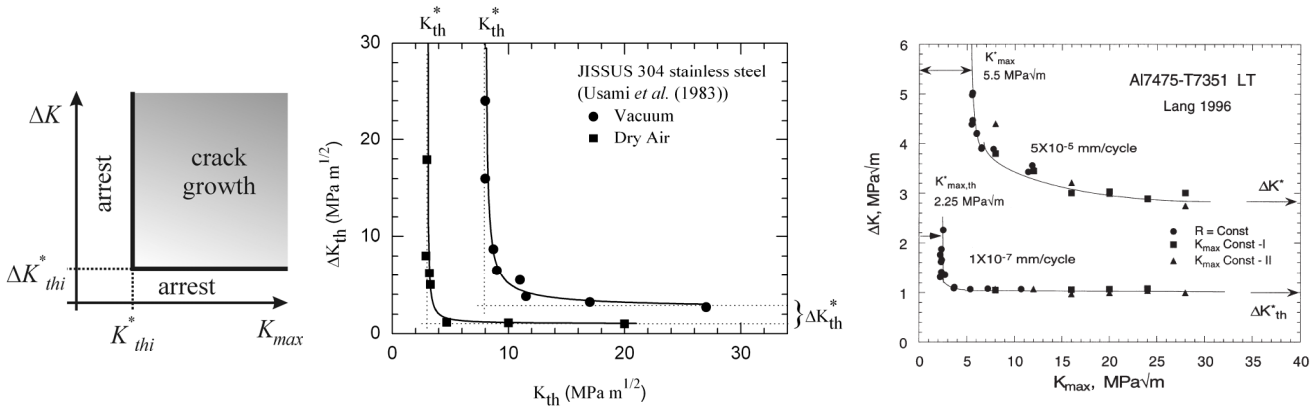

Figure 4: $\Delta K - K_{\max}$ diagram proposed for small cracks (left). Experimental $\Delta K - K_{\max}$ diagram for long cracks for different materials: 304 stainless steel (Usami *et al.* [23]) and Al 7475-T7351 (Lang [24]) (center and right).

SMALL FATIGUE CRACK GROWTH

According to the working assumptions, in the present model the crack growth rate, da/dN, is taken to be a function of the crack tip opening displacement range, *i.e.* $\Delta\phi$. An exponential law can be proposed by analogy with the traditional Paris' law for long cracks, that is,

$$\frac{da}{dN} = B_\sigma \left(\Delta\phi \right)^m \tag{10}$$

where B_σ and m are material constants for a given applied stress, and $\Delta\phi$ is given by Eq. (5). At this stage of the model, no crack closure correction is considered. According to the present fatigue crack propagation description, crack closure may affect the effective range of the applied SIF (or stresses) that assists the crack to overcome the successive microstructural barriers in the material. This fact may contribute to both to decrease the crack growth rate and even the crack arrest.

Fig. 5 illustrates the evolution of da/dN vs. $K_{\max}$ given by Eq. (10) for a small crack under constant amplitude loading. As can be seen, the propagation rate exhibits the typical pattern of decelerations and accelerations due to the successive blocking of CPZ at microstructural barriers in the material. It can also be seen, how the amplitude of the oscillations decrease as the crack increases in length. As expected, the propagation rate exhibits a uniform pattern for long cracks. The figure also depicts the crack propagation rate of a microstructally small crack growing within a grain in the material subjected to a very low applied stress, which is unable to overcome the microstructural barrier and arrest at it. This situation is sometimes referred to as a 'Microstructural Threshold'. On the other hand, the evolution of a long crack is also shown. This case will be discussed in detail in the following section.

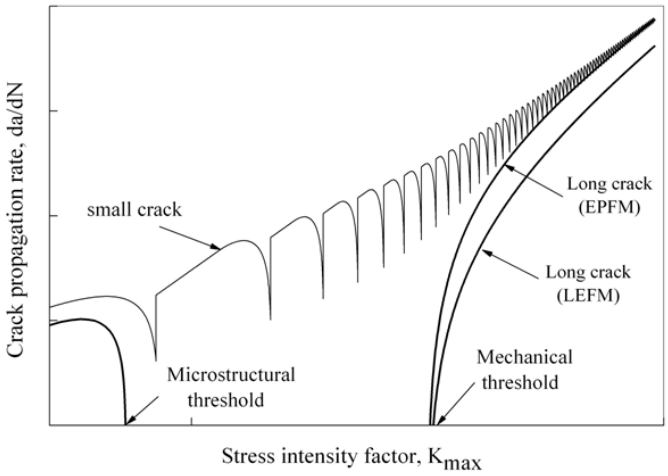

Figure 5: Predicted small crack propagation curve and the EPFM and LEFM curves for long cracks.

In order to illustrate the predictive capability of the present model, Fig. 6 (left) shows the results obtained with the proposed model vs. the experimental data of small cracks obtained by Akiniwa *et al.* [25] for Al 2024-T3 sheets. As can be seen, the experimental trend is nicely captured. A detailed description of the analysis, including fatigue life predictions can be seen in [12].

The current model is also able to predict the effect of the mean stress in fatigue life for unnotched specimens under constant amplitude loading. Fig. 6 (rigth) shows the prediction of the Haigh diagram obtained for Al 2024-T3 for different number of cycles obtained in a recent work still in progress. It can be seen, that the evolution of the iso-fatigue life curves are qualitatively very promising.

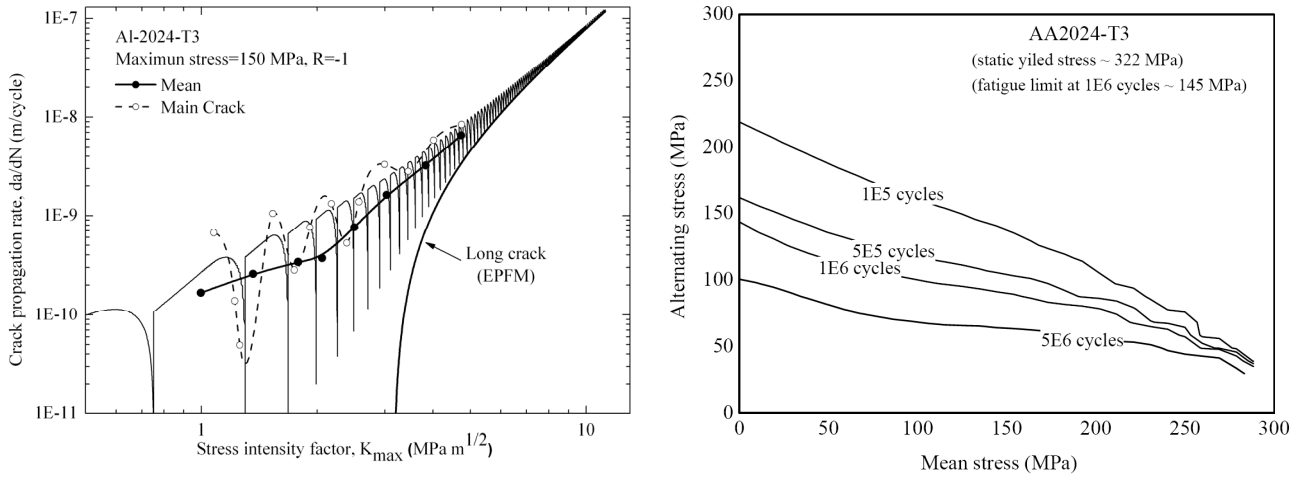

Figure 6: Predicted small crack propagation curve and experimental data for Al 2024-T3 by Akiniwa *et al.* [25] (left). Predicted Haigh's diagram for different fatigue lives.

LONG FATIGUE CRACK GROWTH. TWO-PARAMETER APPROACH

The fatigue crack growth description proposed for small cracks can be extended in a natural way to long crack regime. In fact, long cracks differ from small ones in that they exhibit *microstructural* and *mechanical similitude*. According to Chan and Lankford [20], this refers to the fact that a long crack encompasses such a large number of grains that its fatigue behavior is insensitive to both the microstructure and local mechanical properties from grain to grain.

In the present model a long crack can be represented by making the crack length a, and the position of MPZ and CPZ large enough in relation to the characteristic microstructural size. As can be seen in Fig. 5, the amplitude of oscillations in

crack growth rate reduces substantially in the long crack regime. In terms of the model, this means that, in long crack growth regime, the variation of the dimensionless crack lengths is very small and can be represented by their critical values, that is

$$n_1^{\infty} \approx n_1^{i\to\infty}\Big|_C = \cos\left(\frac{\pi}{2}\frac{\sigma_{\max}}{\sigma_2^{\infty}}\left(1-\frac{K_{th\infty}^*}{K_{\max}}\right)\right) \tag{11}$$

for the ratio crack length to MPZ length, and

$$n_d \approx n_d^{j\to\infty}\Big|_C = \cos\left(\frac{\pi}{2}\frac{\Delta\sigma}{\Delta\sigma_2^{\infty}}\left(1-\frac{\Delta K_{th\infty}^*}{\Delta K}\right)\right) \tag{12}$$

for the ratio crack length to CPZ length. The scrip ∞ refers a long crack. Thus, $K_{th\infty}^*$ and $\Delta K_{th\infty}^*$ are respectively the maximum-controlled and range-controlled SIF thresholds for long cracks. As noted earlier, σ_2^{∞} can be assumed the monotonic yield strength of the material, *i.e.* $\sigma_2^{\infty} \approx \sigma_Y$, and $\Delta\sigma_2^{\infty}$ corresponds with the variation of yield strength to produce reverse yielding, in this case $\Delta\sigma_2^{\infty} \approx 2\sigma_Y$.

Please note that, for SIF values far from the SIF threshold, Eqs. (11) and (12) yield respectively the ratio of the crack length to the position of the MPZ and the CPZ pointed out by the BCS model [19] or Dugdale model [26] for long cracks under elasto-plastic loading conditions. Thus, according to present model, the FCG rate for a long crack in the Elasto-Plastic regime can be readily obtained by setting Eqs. (5) and (10) for long cracks and using the critical conditions given by Eqs. (11) and (12), that is,

$$\frac{da}{dN} = B_\sigma\left(\Delta\phi^{\infty}\right)^m \quad \therefore \quad \Delta\phi^{\infty} = \frac{8}{\pi^2 E'}\frac{\Delta K^2}{\Delta\sigma}\left\{\left(\frac{\Delta\sigma_Y}{\Delta\sigma}\right)\ln\left(\frac{1}{n_d}\right)+\frac{\pi}{2}\frac{\sqrt{1-(n_d)^2}}{n_d}\left[1-\frac{2}{\pi}\left(\frac{\Delta\sigma_Y}{\Delta\sigma}\right)\cos^{-1}n_d\right]\right\}$$

$$n_d \approx n_d^{j\to\infty}\Big|_C = \cos\left(\frac{\pi}{2}\frac{\Delta\sigma}{2\sigma_Y}\left(1-\frac{\Delta K_{th\infty}^*}{\Delta K}\right)\right) \quad \text{(critical condition for CPZ evolution)} \tag{13}$$

$$n_1^{\infty} \approx n_1^{i\to\infty}\Big|_C = \cos\left(\frac{\pi}{2}\frac{\sigma_{\max}}{\sigma_Y}\left(1-\frac{K_{th\infty}^*}{K_{\max}}\right)\right) \quad \text{(critical condition for MPZ evolution)}$$

The trends of Eq. (13) is depicted in Figs. 5 and 6 for $R=-1$. As can be seen, Eq. (13) follows the expected evolution of the classical Elasto-Plastic Fracture Mechanics (EPFM) for long cracks.

The Linear Elastic Fracture Mechanics (LEFM) FCG rate for long cracks can be also obtained simply by imposing small-scale yielding at the crack tip in both MPZ and CPZ. This is attained by setting $n_1^{\infty} \approx n_1^{i\to\infty}\Big|_C \approx 1$ and $n_d \approx n_d^{j\to\infty}\Big|_C \approx 1$ in Eq. (13), which can be simplified as follows

$$\frac{da}{dN} = B_\sigma\left(\Delta\phi^{\infty}\right)^m \quad \therefore \quad \Delta\phi^{\infty} \approx \frac{8}{\pi^2 E'}\frac{\Delta K^2}{\Delta\sigma}\left\{\frac{\pi}{2}\frac{\sqrt{1-(n_d)^2}}{n_d}\right\} \approx \frac{4}{\pi E'}\frac{\Delta K^2}{\Delta\sigma}\sqrt{2\left(1-n_d\right)}$$

$$n_d \approx \cos\left(\frac{\pi}{2}\frac{\Delta\sigma}{2\sigma_Y}\left(1-\frac{\Delta K_{th\infty}^*}{\Delta K}\right)\right) \approx 1 \quad \text{(critical condition for CPZ evolution)} \tag{14}$$

$$n_1^{\infty} \approx \cos\left(\frac{\pi}{2}\frac{\sigma_{\max}}{\sigma_Y}\left(1-\frac{K_{th\infty}^*}{K_{\max}}\right)\right) \approx 1 \quad \text{(critical condition for MPZ evolution)}$$

In view of the fact that $\sqrt{2\left(1-n_d\right)} \approx \cos^{-1}\left(n_d\right)$, the Eq. (14) can be written as

$$\frac{da}{dN} = B_\sigma \left(\Delta\phi^\infty\right)^m \quad \therefore \quad \Delta\phi^\infty \approx \frac{4}{\pi E'}\frac{\Delta K^2}{\Delta\sigma}\cos^{-1}\left(n_d\right)$$

$$n_d \approx \cos\left(\frac{\pi}{2}\frac{\Delta\sigma}{2\sigma_Y}\left(1-\frac{\Delta K^*_{th\infty}}{\Delta K}\right)\right)\approx 1 \qquad \text{(critical condition for CPZ evolution)} \tag{15}$$

$$n_1^\infty \approx \cos\left(\frac{\pi}{2}\frac{\sigma_{\max}}{\sigma_Y}\left(1-\frac{K^*_{th\infty}}{K_{\max}}\right)\right)\approx 1 \qquad \text{(critical condition for MPZ evolution)}$$

Fig. 5 depicts the evolution of Eq. (14) or (15) for $R=-1$. As expected, the EPFM and LEFM curves run almost parallel in the long crack regime due to the effect of the crack tip plasticity.

According to the existence of two independent fatigue thresholds, two different situations can be obtained depending on the relative value of R with respect to R^*, where $R^* = 1-\Delta K^*_{th\infty}/K^*_{th\infty}$ (see. Fig. 4). The value of R^* is ranging from 0.5 to 0.6 for many engineering materials [1, 2]. Thus, if $R \geq R^*$ then the *range-controlled fatigue threshold* $\Delta K^*_{th\infty}$ will be the dominant threshold. This means that the maximum applied SIF will always be high enough to assist MPZ to overcome the microstructural barriers, and will be evolution of the CPZ and its eventual arrest at a microstructural barrier the event that will control the crack propagation. Thus, the FCG curve is obtained by substituting the n_d expression into $\Delta\phi^\infty$ in Eq. (15). On the other hand, when $R < R^*$, the maximum fatigue threshold $K^*_{th\infty}$ will be the dominant threshold. In this situation, the applied SIF range is high enough to assist CPZ to overcome the microstructural barriers, and the eventual arrest of MPZ at certain microstructural barrier and, as a consequence, the latter arrest of the CPZ will govern the crack propagation. Now, the FCG curve can be approximated by assuming $n_d \approx n_1^\infty \approx 1$ in Eq. (15). Thus, the FCG rate in LEFM regime can be expressed as follows

$$\frac{da}{dN} \approx \begin{cases} B_\sigma\left(\dfrac{1}{E'\sigma_Y}\Delta K^2\left(1-\dfrac{\Delta K^*_{th\infty}}{\Delta K}\right)\right)^m & \text{for} \quad R \geq R^* \\ B_\sigma\left(\dfrac{2}{E'\sigma_Y}\Delta K\, K_{\max}\left(1-\dfrac{K^*_{th\infty}}{K_{\max}}\right)\right)^m & \text{for} \quad R < R^* \end{cases} \tag{16}$$

It is interesting to note that Eq. (16) suggests a single-parameter crack driving force based on the range of the applied loads, *e.g.* ΔK, to describe the propagation rate when $R \geq R^*$, and a two-parameter crack driving force based on based on a combination of the maximum and the range of the applied loads, *e.g.* $\Delta K \cdot K_{\max}$, when $R < R^*$. This fact connects fairly well with recent models claiming the use of two-parameter crack driving force to characterize the FCG rate in the long cracks regime [5-10].

CONCLUSIONS

The model presented provides a micromechanical description of small crack propagation based on the successive blocking of the monotonic plastic zone (MPZ) and the cyclic plastic zone (CPZ) of a crack at microstructural barriers of the material. This allows two independent thresholds conditions to be defined. One is related to the capability of the MPZ to overcome the successive microstructural barriers in the material, which depends on the maximum applied load (*maximum-controlled fatigue threshold*). The other is associated to the ability of the CPZ to surmount the microstructural barriers within the MPZ, and is determined by the range of the applied load (*range-controlled fatigue threshold*).

This model covers the long crack regime too. In this case, the two independent thresholds lead the fatigue crack driving force being expressed either via a single-parameter function based on the range of the applied loads, *e.g.* ΔK, or via a two-parameter crack driving force based on based on a combination of the maximum and the range of the applied loads, *e.g.* $\Delta K \cdot K_{\max}$, depending on the R value.

The present model provides a plausible and unified description of the fatigue crack growth process consistent with the experimental evidence, and connecting the small and long crack regime in a natural manner.

REFERENCES

[1] A.K. Vasudevan, K. Sadananda, N. Louat, Scripta Metallurgica et Materialia, 28 (1993) 65.
[2] A.K. Vasudevan, K. Sadananda, N. Louat, Materials Science and Engineering A, 188 (1994) 1.
[3] A.K. Vasudevan, K., Sadananda, G. Glinka, Int. J. Fatigue, 23 (2001) S39.
[4] M.N. James, L. Wenfong, Materials Science and Engineering A, 265 (1999) 129.
[5] R.O. Ritchie, B. L. Boyce, J.P. Campbell, O. Roder, A.W. Thompson, W.W. Milligan, Int. J. Fatigue, 21 (1999) 653.
[6] D. Kujawski, Int J Fatigue, 23 (2001) 733.
[7] S. Dinda, S, D. Kujawski, Eng. Fract. Mech., 71 (2004) 1779.
[8] S. Stoychev, D. Kujawski, Int. J. Fatigue, 27 (2005) 1425.
[9] A.H. Noroozi, G. Glinka, S. Lambert, Int. J. Fatigue, 27 (2005) 1277.
[10] A.H. Noroozi, G. Glinka, S. Lambert, Engng. Fract. Mech., 75 (2008) 188.
[11] A. Shyam, J.E. Allison, C.J. Szczepanski, T.M. Pollok, J.W. Jones, Acta Materialia, 55 (2007) 6606.
[12] C. Vallellano, J. Vazquez, A. Navarro, J. Dominguez, Fatigue Fract. Engng. Mat. Struct., 32 (2009) 515.
[13] Navarro, E.R. de los Rios, Phil. Mag., 57 (1988) 15.
[14] Navarro, E.R. de los Rios, Phil. Mag., 57 (1988) 37.
[15] Navarro, E.R. de los Rios, Proc. R. Soc. Lond. A, 437 (1992) 375.
[16] S Taira, K Tanaka, Y. Nakai, Mech. Res. Commun. 5 (1978) 375.
[17] K. Tanaka, Y. Akiniwa, Y. Nakai, R.P. Wei, Engng. Fract. Mech. 24 (1986) 803.
[18] Vallellano, A. Navarro, J. Dominguez, Phil. Mag. A, 82 (2002) 81.
[19] B.A. Bilby, A.H. Cottrell, K.H. Swinden, Proc. Royal Soc. A, 272 (1963) 304.
[20] K.S. Chan, J. Lankford, Acta Metall., 36 (1988) 193.
[21] Vallellano, A. Navarro, J. Dominguez, Fatigue Fract. Engng. Mat. Struct., 23 (2000) 113.
[22] Vallellano, A. Navarro, J. Dominguez, Fatigue Fract. Engng. Mat. Struct., 23 (2000) 123.
[23] S. Usami, Y. Fukuda and S. Shida, In: Proc. 4th National Congress on Pressure Vessel Technology, ASME Publication, (1983) 1.
[24] M. Lang., PhD. Dissertation, Institue fur Werkstoff-Forschung, (1996).
[25] Y. Akiniwa, K. Tanaka, E. Matsui, Mat. Sci. Engng. A, 104 (1988) 105.
[26] D.S. Dugdale, J. Mech. Phys. Sol., 8 (1960) 100.